

# **SURFACE PEGYLATION AND PASYLATION TO REGULATE NANOPARTICLE INTERACTIONS WITH BIOLOGICAL ENVIRONMENT**

**BARBORA TESAROVA<sup>1,2</sup>, SIMONA DOSTALOVA<sup>1,2</sup>, DAVID HYNEK<sup>1,2</sup>,  
VOJTECH ADAM<sup>1,2</sup>, ZBYNEK HEGER<sup>1,2</sup>**

<sup>1</sup> Department of Chemistry and Biochemistry

Mendel University in Brno

Zemedelska 1, 613 00 Brno

<sup>2</sup> Central European Institute of Technology

Brno University of Technology

Purkynova 123, 612 00 Brno

CZECH REPUBLIC

tesarova.barca@seznam.cz

**Abstract:** Many researchers are developing nanocarriers in order to minimize side effects of cytotoxic drugs during cancer treatment *via* chemotherapy. Nanocarriers can serve as a suitable platform for targeted drug delivery. To overcome their failure in *in vivo* use, the effects of surface modifications (PEGylation and PASylation) of natural nanocarriers based on apoferritin were tested in this work. Various properties of these modified apoferritin nanoparticles were studied, such as their size or degree of hemolysis. TEM characterization was also performed. The formation of hard coronas on these particles in plasma environment was evaluated using SDS-PAGE electrophoresis. The best biocompatibility results were obtained using apoferritin nanoparticles with PEG surface modification.

**Key Words:** apoferritin; nanomedicine; protein coronas; surface modifications

## **INTRODUCTION**

Nowadays there are over 200 different types of cancer affecting humans (Broto et al. 2017). Chemotherapy is a method for treating cancer using cytotoxic agents, whose main disadvantage is their non-specificity for cancer cells. This means that they are also strongly affecting healthy cells. Thus, the actual dose of cytostatic received by affected tissue is hard to control (Broto et al. 2017). By targeting of cytostatics directly to diseased tissue, it is possible to minimize the serious side effects of chemotherapy, such as the cardiotoxicity of doxorubicin or mutagenicity of ellipticine (Bazak et al. 2015). The number of nanocarriers that could be used for this purpose is growing exponentially, but only a few of these nanocarriers are currently tested in clinical trials and even lower number is used in clinical practice. To improve the success of their therapeutic use, a better understanding of their biological identity is needed. Many nanoconstructs cannot fulfil their role after exposition to body environment; they can even lead to hemolysis or aggregation of blood platelets. Or, upon entering blood stream, nanoparticles are often coated by protein corona, changing their surface, and hampering their internalization into diseased cells. Protein corona forms after exposure of nanocarrier to plasma proteins that occur at 60-80 g/l (Broto et al. 2017). We can define protein corona as a natural interface between nanomaterials and living matter in biological milieu (Monopoli et al. 2013).

In order to control and reduce the binding of additional biomolecules and formation of protein corona, surface modifications with various polymers can be used. In this contribution, we studied the effects of modification with poly-ethylene glycol (PEGylation) and peptides rich in proline, alanine and serine residues (PASylation). PEGylation represents chemical conjugation with synthetic hydrophilic and uncharged synthetic polymer PEG (Binder and Skerra 2017). This usually happens *via* the  $\epsilon$ -amino group of lysine residues or the thiol group of cysteine. PEGylation is the most widely established method of prolonging the half-life of drug in bodily fluids (Pasut and Veronese 2012).

To this date, there are up to 15 approved PEGylated drugs (Gabizon et al. 2016). The main drawbacks of using PEG for surface modification are its high cost, non-biodegradability and possible cellular vacuolation caused by PEG (Ivens et al. 2015). PASylation is a biological alternative to PEGylation based on genetic fusion or chemical coupling of nanoparticles with polypeptides (Chow et al. 2008). PASylation bypasses disadvantages of PEGylation, such as its high cost and polydispersity. Moreover, PAS has lower viscosity and is more hydrophilic than PEG, which enables intravenous administration of PASylated drugs or nanoparticles (Binder and Skerra 2017). Their most important features are their non-immunogenicity (Harari et al. 2014), stability in plasma (Kuhn et al. 2016) and quick degradation by intracellular/lysosomal proteases after cellular uptake, which does not cause cellular vacuolization (Binder and Skerra 2017).

The effects of PEGylation and PASylation on *in vivo* behaviour of nanoparticles were studied using ubiquitous protein cage apoferritin (Apo) with encapsulated ellipticine (Elli). Apo self-assembles into hollow rhombic dodecahedral cage of 12 nm in diameter, which stores and transports iron and iron ions in organism (Bulvik et al. 2012). Ellipticine is a natural pyridocarbazole type alkaloid showing cytotoxic activity against many cancer cell lines but it is highly mutagenic, which can be risky for healthy cells (Kizek et al. 2012). We encapsulated Elli into Apo and modified its surface with PEG or PAS sequences. The characterization of these nanoformulations was performed *via* dynamic light scattering (DLS) and transmission electron microscopy (TEM). The behaviour of these nanoparticles in human blood was evaluated using SDS-PAGE electrophoresis and hemolytic assay.

## MATERIAL AND METHODS

### Chemicals

All chemicals of ACS purity were obtained from Sigma-Aldrich (St. Louis, MO, USA).

### Encapsulation of Elli into Apo

The stock solution of ellipticine with concentration of 1 mg/ml was prepared by dissolving Elli in 1 M HCl and deionized water in ratio 1 : 150. For each sample, 200 µl of 1 mg/ml Elli was added to 100 µl of deionized water and 20 µl of 50 mg/ml horse spleen Apo and gently mixed for 15 min. To reassemble the Apo structure disassembled by acidic Elli and encapsulate Elli in Apo cavity, 0.66 µl of 1 M sodium hydroxide solution was added and the samples were mixed for further 15 min. To filter out non-encapsulated Elli, solution exchange was performed three times (centrifugation at 6000 g for 15 min).

### Surface modification with PEG

50 µl of 10 mM PEG maleimide in PBS (phosphate buffered saline, pH 7.4: 0.137 M NaCl + 0.0027 M KCl + 0.0014 M KH<sub>2</sub>PO<sub>4</sub> + 0.0043 M Na<sub>2</sub>HPO<sub>4</sub>) and 629 µl of PBS was added to ApoElli and mixed for 1 h. To filter unbound PEG, the sample was 5 times diafiltrated using Amicon® Ultra 0-5 ml 50K Merck Millipore (Billerica, MA, USA) at 6000 g for 15 min.

### Surface modification with PAS

25 µl of 1.3 nm gold nanoparticles was added to ApoElli and the samples were mixed for 14 h to allow binding of Au nanoparticles on the surface of ApoElli nanoparticles (creating ApoElli-Au). Solution exchange was performed two times to remove unbound Au nanoparticles. 3 µl of 1.25 mg/ml PAS-10 (ASPAAPAPASC) and PAS-20 (ASPAAPAPASPAAPSAPAC) was added to ApoElli-Au and the samples were incubated for 1 h at 45 °C to allow binding of cysteine to gold. Then, solution exchange was performed to remove unbound molecules of PAS peptides.

### Characterization of prepared samples

#### *Concentration of encapsulated Elli*

The concentration of encapsulated Elli was evaluated by absorbance measurement at 420 nm using Tecan Infinite 200 PRO (Männedorf, Switzerland).

### *Size characterization by DLS*

The average size of prepared nanoparticles was determined by quasielastic dynamic light scattering using Zetasizer Nano ZS instrument, Malvern Instruments Ltd. (Worcestershire, UK). Polystyrene latex cells ZEN0040 were used for measurements and the conditions of measurements were as follows: detector angle of 173°, wavelength of 633 nm and temperature of 25 °C, equilibration time 120 s. The measurements were performed in hexaplicates.

### *TEM characterization*

Visualization of nanocarriers and their surface modification was performed using transmission electron microscopy (TEM) with negative staining technique. An organotungsten compound Nano-W Nanoprobes (Yaphank, NY, USA) was used. 4 µ of samples were deposited onto 400-mesh copper grids coated with a continuous carbon layer. Dried grids were imaged by TEM Tecnai F20; FEI, (Hillsboro, OR, USA).

### ***In vitro evaluation of behaviour in human blood***

Blood samples were collected into EDTA coated Vacutainer tubes and centrifuged at 3 000 rpm and 25 °C for 10 min. Red blood cells (RBC) were used for hemolytic assay while pooled plasma was further centrifuged at 22 000 rcf and 4 °C and for 30 min and used to evaluate formation of protein corona.

### *Hard corona formation*

100 µl of plasma was mixed with 100 µl of 200 µg/ml Elli, either free or encapsulated in modified and unmodified Apo nanocarrier. The samples were incubated at 600 rpm and 37 °C for 35 min. To remove unbound plasma proteins from nanoparticles, 4 times solution exchange was performed. To determine the degree of protein corona formed on tested nanoformulations, SDS-PAGE electrophoresis was used. Proteins were separated at 200 V for 35 min using 12.5% polyacrylamide gel.

### *Hemolysis assay*

RBC were centrifuged at 3 000 rpm for 10 min multiple times and resuspended in 150 mM NaCl until the supernatants were transparent. Then, RBCs were diluted with PBS and 150 µl was mixed with 150 µl of decreasing concentrations of Elli (100; 50; 25; 12.5 and 6.3 µg/ml), either free or encapsulated in Apo nanoformulations; negative control (PBS) or positive control (0.2% Triton X-100). The samples were incubated at 37 °C and 600 rpm for 1 h. Incubation was followed by centrifugation at 3 000 rpm for 10 min. Absorbance at 540 nm was measured and the percentage of hemolysis was calculated *via* following formula:

$$\% \text{hemolysis} = [(A_t - A_c)/(A_{100\%} - A_c)] \cdot 100 \quad (1)$$

where  $A_t$  stands for absorbance of sample's supernatant,  $A_c$  represents absorbance of negative control's supernatant,  $A_{100\%}$  stands for absorbance of positive control's supernatant.

## **RESULTS AND DISCUSSION**

### **Characterization of prepared samples**

#### *Elli encapsulation efficiency, size characterization by DLS*

The highest encapsulation efficiency (9%) was achieved in sample with PEG modification (Table 1). The size measurements (Table 1) showed that the size of Apo increased from 12 nm to 18 nm after encapsulation of Elli. The various surface modifications further influenced the size of ApoElli, where PAS-10 modification caused aggregation of multiple ApoElli molecules while PAS-20 and PEG modifications did not cause any aggregation.

Table 1 Characterization of prepared nanoparticles

Number	Sample	Encapsulation efficiency [%]	Size of prepared nanoparticles [nm]
	Surface modification		
1	PEG	91.20	13.545
2	PAS-10	52.83	79.671
3	PAS-20	43.96	13.545
4	No surface modification	69.00	18.166

*TEM characterization*

TEM characterization was performed to detect changes in apoferritin structure after surface modifications (Figure 1). The results showed that the tested surface modifications did not cause disassembly of Apo quaternary structure, as typical icosahedral particles were observed in all samples. The presence of polymer on ApoElli surface can be seen in PEGylated samples. PASylation was also proven by thicker protein shell of ApoElli.

Figure 1 TEM images, scale corresponds to 25 nm (from left to right: apoferritin modified with PEG; apoferritin modified with PAS-10; apoferritin modified with PAS-20; control without any surface modification)

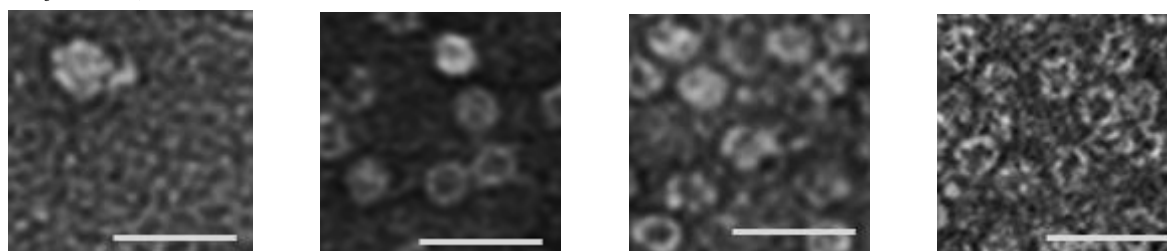
*Hemolysis assay*

Table 2 Degree of hemolysis caused by all tested formulations

Concentration of Elli [μg/ml]	PEG	PAS-10	PAS-20	No surface modification	Elli
100.00	0.05	0.00	0.00	0.06	5.41
50.00	0.00	0.00	0.00	0.00	3.74
25.00	0.00	0.00	0.00	0.00	1.67
12.50	0.00	0.00	0.00	0.00	0.84
6.25	0.00	0.00	0.00	0.00	0.15

To evaluate hemotoxicity of the tested nanoparticles, RBC hemolytic assay was performed. The results of hemolytic assay are summarized in Table 2. The lysed RBC caused red coloring of the supernatant, whereas transparent supernatant showed no occurring hemolysis. Free Elli caused hemolysis at all tested concentrations (see Figure 2) and the degree of hemolysis was dependent on Elli concentration (5% at 100 μg/ml). The encapsulation of Elli in Apo nanocarrier favorably influenced this hemolysis caused by Elli. Very low degree of hemolysis was observed only at highest Elli concentration in samples containing PEGylated ApoElli and sample without any surface modification (0.05% for PEGylated ApoElli and 0.06% for ApoElli). Samples with surface modified with PAS-10 (see Figure 3) and PAS-20 did not show any degree of hemolysis. The obtained results clearly show that all ApoElli nanoformulations, both unmodified and surface modified, are highly biocompatible with human RBC.

Figure 2 Samples without using apoferritin nanocarrier (from left to right: negative control; 6.25; 12.5; 25; 50 and 100  $\mu\text{g/ml}$  Elli; positive control)

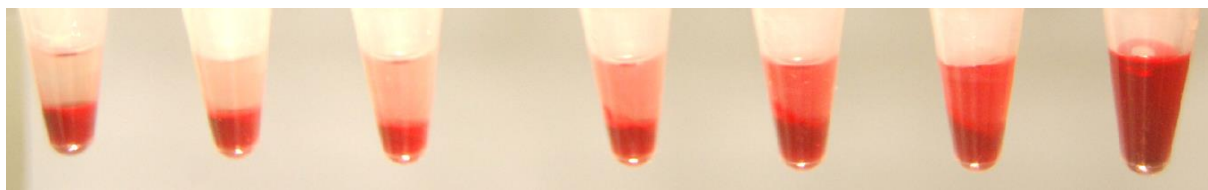
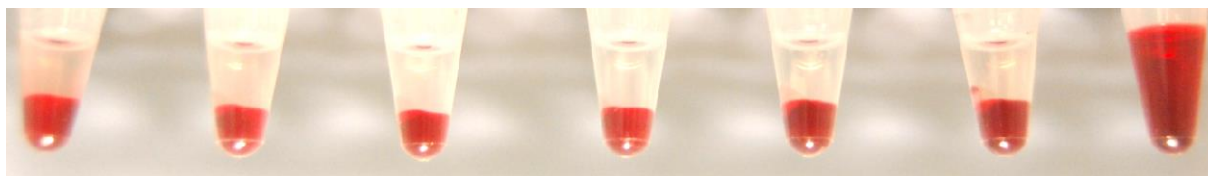


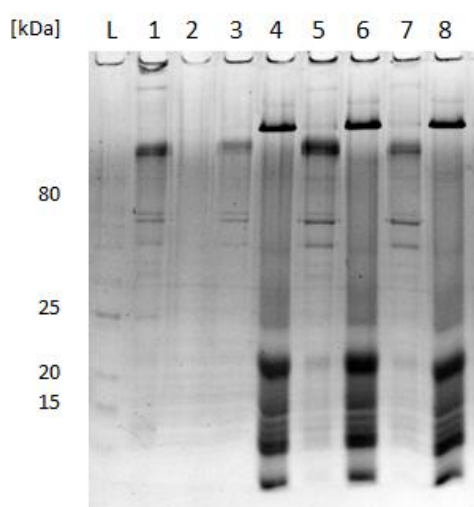
Figure 3 Samples modified with PAS-10 (from left to right: negative control; 6.25; 12.5; 25; 50 and 100  $\mu\text{g/ml}$  Elli encapsulated in Apo modified with PAS-10; positive control)



#### Evaluation of protein coronas

We further performed SDS-PAGE in order to evaluate the influence of PEGylation and PASylation on the formation of protein corona on ApoElli surface (see Figure 4). The ideal surface modification of nanocarrier should minimize interactions between the surface of nanocarrier and plasma proteins, which naturally occur in human plasma. Efficient surface modification would reduce binding of proteins on the surface of nanocarrier, which leads to reduced protein corona formation or even inhibits protein corona formation all together. The surface modification with PAS-10 and PAS-20 did not decrease the interactions with plasma proteins and the protein corona was formed in a very similar way to that formed around unmodified ApoElli. Thus it can be concluded, that these modifications were not suitable for surface modifications of nanocarriers in order to avoid protein-nanocarrier interactions in bodily fluids. On the other hand, PEGylated ApoElli showed presence of no proteins from human plasma. Surface modification with PEG proved more suitable for future *in vivo* use as it was able to significantly lower protein-nanocarrier interactions.

Figure 4 SDS-PAGE (L - NEB Protein Ladder 10-250 kDa; 1 - PEGylated ApoElli; 2 - protein corona on PEGylated ApoElli; 3 - PAS-10ylated ApoElli; 4 - protein corona on PAS-10ylated ApoElli; 5 - PAS-20ylated ApoElli; 6 - protein corona on PAS-20ylated ApoElli; 7 - ApoElli; 8 - protein corona on ApoElli)





## CONCLUSION

The experiment presented in this work dealt with the prediction of *in vivo* behaviour of apoferritin nanocarrier, based on *in vitro* tests of their hemotoxicity and formation of protein corona around these particles in human plasma environment. The surface of this apoferritin nanocarrier was modified with polymer (PEG) and peptides (PAS) in order to decrease these negative interactions. Overall, the results showed that while all tested modifications favourably influenced unwanted hemotoxicity of ellipticine, only PEGylation was able to lower interactions between nanocarrier surface and proteins in bodily fluids.

## ACKNOWLEDGEMENTS

The research was financially supported by the Grant Agency of the Czech Republic (GA CR 17-12816S) and CEITEC 2020 (LQ1601).

## REFERENCES

- Bazak, R., Houri, M., El Achy, S., Kamel, S., Refaat, T. 2015. Cancer active targeting by nanoparticles: a comprehensive review of literature. *Journal of Cancer Research and Clinical Oncology*, 141(5): 769–84.
- Binder, U., Skerra, A. 2017. PASylation®: A versatile technology to extend drug delivery. *Current Opinion in Colloid & Interface Science*, 31:10–17.
- Broto, M., Galve, R., Marco, M.P. 2017. Bioanalytical methods for cytostatic therapeutic drug monitoring and occupational exposure assessment. *TrAC Trends in Analytical Chemistry*, 93: 152–170.
- Bulvik, B.E., Berenshtein, E., Meyron-Holtz, E.G., Konijn, A.M., Chevion, M. 2012. Cardiac protection by preconditioning is generated via an iron-signal created by proteasomal degradation of iron proteins. *PloS One*, 7(11): 1–14.
- Chow, D., Nunalee, M.L., Lim, D.W., Simnick, A.J., Chilkoti A. 2008. Peptide-based Biopolymers in Biomedicine and Biotechnology. *Materials Science & Engineering*, 62(4): 125–155.
- Gabizon, A.A., Patil, Y., La-Beck, N.M. 2016. New insights and evolving role of pegylated liposomal doxorubicin in cancer therapy. *Drug Resistance Updates: Reviews and Commentaries in Antimicrobial and Anticancer Chemotherapy*, 29: 90–106.
- Harari, D., Kuhn, N., Abramovich, R., Sasson, K., Zozulya, A.L., Smith, P., Schlapschy, M., Aharoni, R., Koster, M., Eilam, R., Skerra, A., Schreiber, G. 2014. Enhanced *in vivo* efficacy of a type I interferon superagonist with extended plasma half-life in a mouse model of multiple sclerosis. *The Journal of Biological Chemistry*, 289(42): 29014–29029.
- Ivens, I.A., Achanzar, W., Baumann, A., Brandli-Baiocco, A., Cavagnaro, J., Dempster, M., Depelchin, B.O., Rovira, A.R., Dill-Morton, L., Lane, J.H., Reipert, B.M., Salcedo, T., Schweighardt, B., Tsuruda, L.S., Turecek, P.L., Sims, J. 2015. PEGylated Biopharmaceuticals: Current Experience and Considerations for Nonclinical Development. *Toxicologic Pathology*, 43(7): 959–83.
- Kizek, R., Adam, V., Hrabeta, J., Eckschlager, T., Smutny, S., Burda, J.V., Frei, E., Stiborova, M. 2012. Anthracyclines and ellipticines as DNA-damaging anticancer drugs: recent advances. *Pharmacology & Therapeutics*, 133(1): 26–39.
- Kuhn, N., Schmidt, C.Q., Schlapschy, M., Skerra, A. 2016. PASylated Coversin, a C5-Specific Complement Inhibitor with Extended Pharmacokinetics, Shows Enhanced Anti-Hemolytic Activity *in Vitro*. *Bioconjugate Chemistry*, 27(10): 2359–2371.
- Monopoli, M.P., Pitek, A.S., Lynch, I., Dawson, K.A. 2013. Formation and characterization of the nanoparticle-protein corona. *Methods in Molecular Biology*, 1025: 137–55.
- Pasut, G., Veronese, F.M. 2012. State of the art in PEGylation: the great versatility achieved after forty years of research. *Journal of Controlled Release*, 161(2): 461–472.